Progress In Electromagnetics Research C, Vol. 85, 247–257, 2018

Dual-Band Modified Circular Slot Antenna for WLAN and WiMAX Applications

Som Pal Gangwar[1, *], Kapil Gangwar[2], and Arun Kumar[3]

Abstract—In this article, design and analysis of a modified circular slot antenna is discussed. The proposed antenna design is attractive because of two important reasons: (i) modified circular slot creates dual operating bands; (ii) stable radiation characteristics over the operating frequency bands are observed. The complete analysis of proposed radiator has been done on Ansys HFSS simulation software. For verifying the simulated outcomes, a prototype of antenna structure is fabricated and tested. Measured results show that the proposed antenna operates over two frequency bands, i.e., 2.88–3.92 GHz and 5.26–6.28 GHz with the fractional bandwidths of 31% and 17% respectively. Experimentally measured average gain of the proposed radiator is 3 dBi and 6 dBi in lower and upper frequency bands, respectively. All these features of the proposed antenna make it appropriate for WiMAX (3.5 GHz) and WLAN (5.8 GHz) applications.

1. INTRODUCTION

Current age of wireless communication requires low profile, light weight, low cost, easy fabrication and compact radiators. Slot as well as patch antenna is the most suitable one for this purpose. However, these antennas (in their conventional form) also suffer from several shortcomings such as low gain and narrow bandwidth [1]. A lot of research has been done to remove these drawbacks. Slot radiators have the inherent property of giving omnidirectional pattern in one of its principal planes which is not possible in the case of conventional patch antenna [2]. That is why slot antenna is more preferable than microstrip radiators.

Recently, researchers have widely concentrated on multiband characteristics in antennas. It is due to two important reasons: (i) single antenna can work for multiple frequency bands; (ii) band rejection provides better signal to noise ratio [3]. Initially, different techniques were used to obtain dual-band features such as use of different shape slot, i.e., a cross slot [4], a circular slot [5], a square slot [6], and an offset circular slot [7]. A dual-frequency microstrip antenna was proposed in the year 2011. Impedance bandwidths of 26.2% and 22.2% at lower and higher operating bands were obtained by employing an offset microstrip-fed line and a strip close to the radiating edges in the circular slot patch. Its size ($108 \times 108 \times 1.6\,\text{mm}^3$) is larger than the proposed antenna structure [8]. A helix-shaped slot radiator was proposed for dual-band applications. This radiator is applicable to GPS L_1 and L_2 frequency bands, but it suffers from large antenna size [9]. In the year 2016, a cavity backed slot antenna for dual-band applications was proposed. The concept of spurline makes the antenna design more complex [10]. Just after it, a split ring resonator loaded square slot antenna was proposed for dual-frequency applications. The performance of this antenna is very good in terms of bandwidth and gain, but it also suffers from large antenna size [11]. Recently, a very simple dual-band slot antenna design was proposed. It contains

Received 18 June 2018, Accepted 16 July 2018, Scheduled 26 July 2018
* Corresponding author: Som Pal Gangwar (gangwar_sp@rediffmail.com).
[1] Department of Electronics Engineering, KNIT, Sultanpur (UP), India. [2] Department of Electronics Engineering, IIT (ISM), Dhanbad (Jharkhand), India. [3] Department of E & C Engineering, SET, IFTM University, Moradabad (UP), India.

two rectangular slots with offset between them. This antenna is also applicable to WLAN and WiMAX applications. However, its size ($60 \times 60 \times 1.6\,\text{mm}^3$) is larger than the proposed antenna structure [12].

This article presents a modified circular shaped slot antenna for dual-frequency applications. An asymmetrical microstrip line is used to feed the proposed slot antenna. This antenna structure is designed for two frequency bands, i.e., 2.88–3.92 GHz and 5.26–6.28 GHz. It provides stable far-field characteristics with average gains of 3.0 dBi and 6.0 dBi in lower and upper frequency bands, respectively. For better representation, the present article is divided into four different sections (except introduction): (i) geometrical layout of antenna; (ii) analysis of the effect of different antenna parameters; (iii) experimental outcomes; and (iv) conclusion.

2. DESIGN OF ANTENNA GEOMETRY

The top and bottom views of the proposed fabricated antenna are shown in Figure 1. The antenna structure is designed, simulated and then fabricated on a glass epoxy FR-4 substrate having thickness h, relative permittivity ε_r and loss tangent $\tan\delta$.

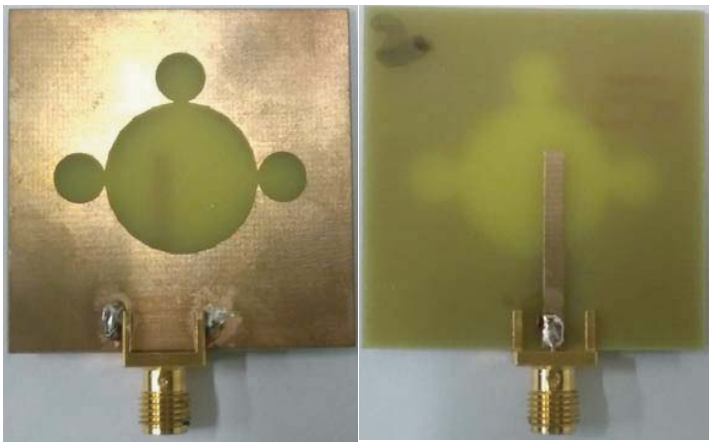

(a) (b)

Figure 1. Fabricated antenna. (a) Top view. (b) Bottom view.

The proposed antenna is printed on both sides of the single substrate. On one side of the square substrate, one circular slot of radius R_1 and three circular slots of radius R_2 each are etched. The bigger circular slot of radius R_1 connects the other three smaller circular slots of radius R_2, as shown in Figures 1 & 2. On the other side of the substrate, the rectangular microstrip line of dimension $L_2 \times W_2$ is printed to feed the antenna. Figure 2 displays the geometrical layout of the proposed antenna structure.

3. ANTENNA ANALYSES

The resonant frequency (f_r) of a circular patch microstrip antenna for the dominant mode TM_{11} mode can be expressed as [1] —

$$(fr)_{11} = \frac{1.8412c}{2\pi R_e\sqrt{\varepsilon_r}} \tag{1}$$

where c is the velocity of light in free space; ε_r is the dielectric constant of substrate; and R_e is the effective radius of patch. The effective radius (R_e) has been introduced to account for the fringing fields along the edge of the resonator, and it is given by [1] —

$$R_e = R\left\{1 + \frac{2h}{\pi R\varepsilon_r}\left[ln\left(\frac{\pi R}{2h}\right) + 1.7726\right]\right\}^{1/2} \tag{2}$$

where R is the physical radius of the circular patch.

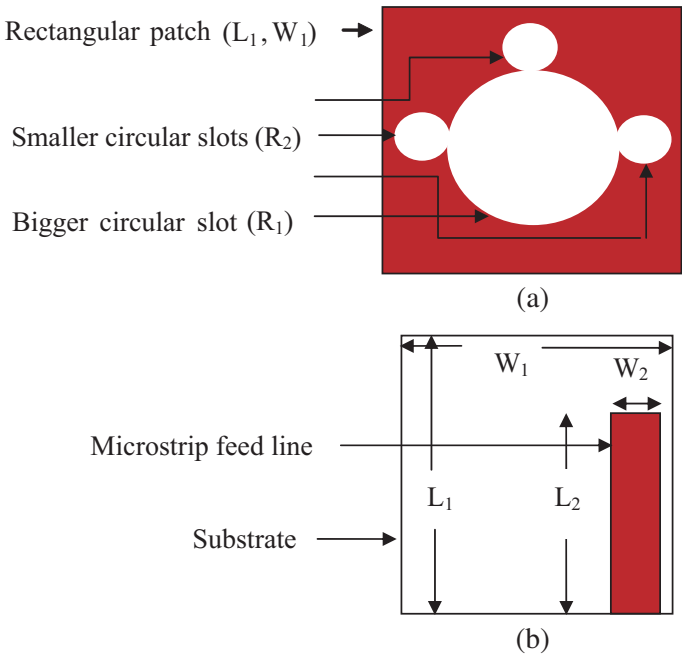

Figure 2. Geometry of proposed antenna. (a) Top view. (b) Bottom view.

By selecting various sizes of the circular slots in the patch, the fundamental resonant mode TM_{11} for an unslotted circular patch microstrip antenna can be split into two separate resonant modes close to each other, and the antenna exhibits characteristics of a dual-band antenna [5, 6, 8].

In order to study the effects of different parameters on the performance of proposed antenna, parametric analysis is performed. When the effect of one parameter is studied, the other parameters are kept constant. The parametric observations provide valuable suggestions for the designing of practical antennas. The parametric analysis of the proposed antenna is performed to get optimized dimensions of antenna and feed element. Table 1 shows the optimized parameters of the proposed antenna. The step by step design of the proposed antenna is shown in Figure 3. The return loss analysis of different design stages (which is shown in Figure 3) is shown in Figure 4.

The observations obtained from Figure 4 are described as follows: when only one circular slot of radius R_1 is etched (design 1), the antenna does not resonate over the operating frequency range. Now, one big circular slot of radius R_1 and one small circular slot of radius R_2 are etched (design 2), and the antenna behaves as a single band antenna and resonates at 3.1 GHz. When one big circular slot and

Table 1. Optimized parameters of proposed antenna.

Parameters	**Unit**
Length of substrate/patch (L_1)	40 mm
Width of substrate/patch (W_1)	40 mm
Length of microstrip line (L_2)	23.5 mm
Width of microstrip line (W_2)	2.5 mm
Radius of bigger circle (R_1)	9 mm
Radius of smaller circles (R_2)	3 mm
Thickness of substrate (h)	1.6 mm
Loss tangent of dielectric constant ($\tan\delta$) = 0.0148 Dielectric constant of substrate $\epsilon_r = 4.4$	

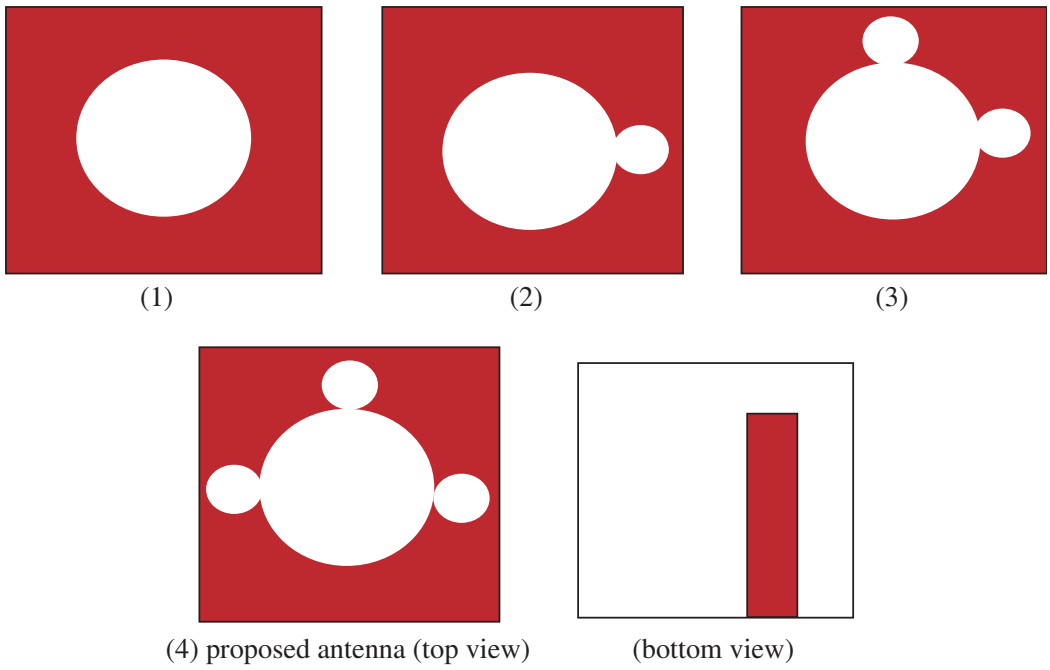

Figure 3. Step by step design of proposed antenna.

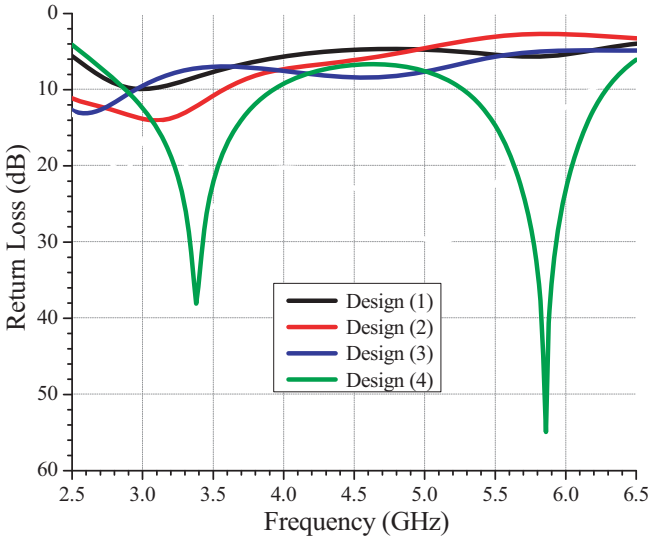

Figure 4. Return loss versus frequency curve for different designs.

two small circular slots are etched in the patch (design 3), the antenna is a single band antenna having resonant frequency of 2.5 GHz with return loss of 14 dB. When one big circular slot and three small circular slots are etched in the patch (design 4), the antenna behaves as a dual-band antenna. This antenna (design 4) has two resonant frequencies 3.38 GHz and 5.86 GHz with return losses of 38.1 dB and 54.9 dB, respectively.

The variation of return loss with movement of position of microstrip line feed from center towards right is shown in Figure 5(a). Feed position is measured from the center of the substrate. Thus, feed positions 1, 2 and 3 mean the the positions of feed are 1.75 mm, 2.25 mm and 2.75 mm right from center, respectively. As shown in Figure 5(a), the variation in feeder position has negligible effect on lower resonant frequency f_1 but has a significant effect on higher resonant frequency f_2. When position

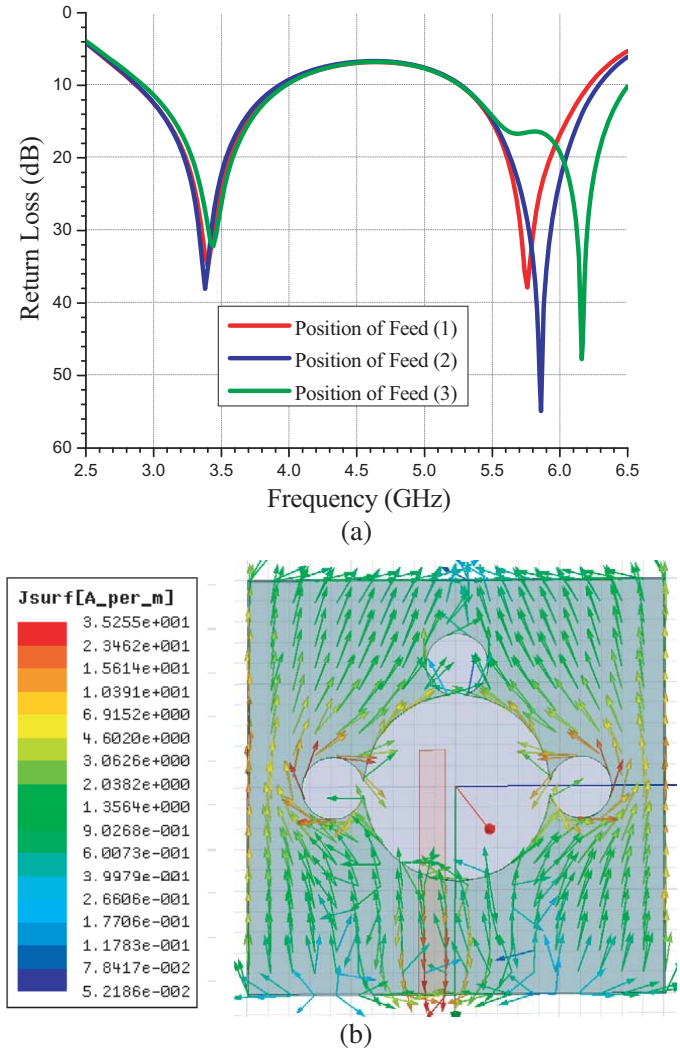

Figure 5. (a) Return loss with variation in position of feed. (b) Surface current density variation.

of feed is (2), maximum coupling exists between feed line and smaller circular slots. It can be verified by surface current density variations of the proposed antenna which is shown in Figure 5(b).

Figure 6 shows variation of return loss for different values of length of feed (L_2). As L_2 decreases from 24 mm to 23.5 mm, f_1 & f_2 shifts towards higher side significantly, and return loss increases significantly at both f_1 & f_2. As L_2 further decreases from 23.5 mm to 23 mm, f_1 & f_2 shift towards higher side marginally, but return loss decreases significantly at both f_1 & f_2. The length of the feed should be greater than or equal to quarter-wavelength, i.e., $L_2 \geq \lambda/4$. Initially, the proposed antenna is designed for center frequency 3.2 GHz, for which $\lambda/4 = 23.4375$ mm. So, we have chosen $L_2 = 23.5$ mm.

Figure 7 shows variation of return loss for different values of radius of bigger circle (R_1). As R_1 increases from 8 mm to 9 mm, f_1 and f_2 shift towards lower side marginally, and return loss increases significantly. As R_1 further increases from 9 mm to 10 mm, f_1 and f_2 shift towards lower side marginally, but return loss decreases significantly. When the bigger circular slot radius is less than 8 mm, no good excitation of two separate resonant modes in the vicinity of the fundamental resonant modes TM_{11} of the corresponding unslotted circular patch antenna can be observed, i.e., no dual-frequency operation can be achieved. When the slot radius is within the range of 8–10 mm, good excitation of two separate resonant modes can be easily achieved by using a single microstrip feed. Better results are obtained for $R_1 = 9$ mm.

Figure 8 shows variation of return loss for different values of radius of smaller circle (R_2). As

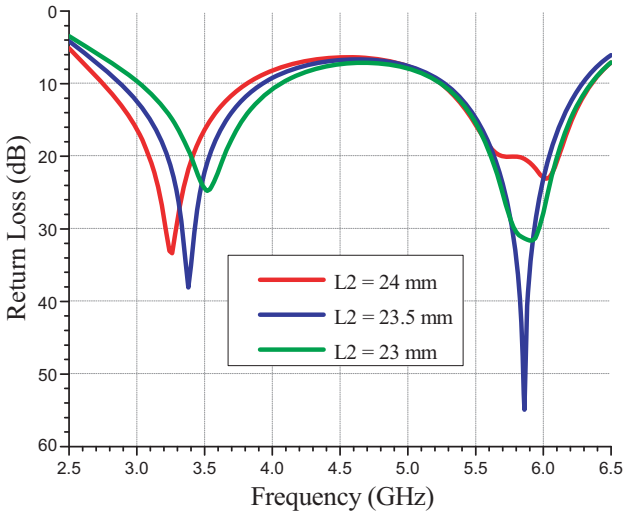

Figure 6. Return loss with variation in length of feed (L_2).

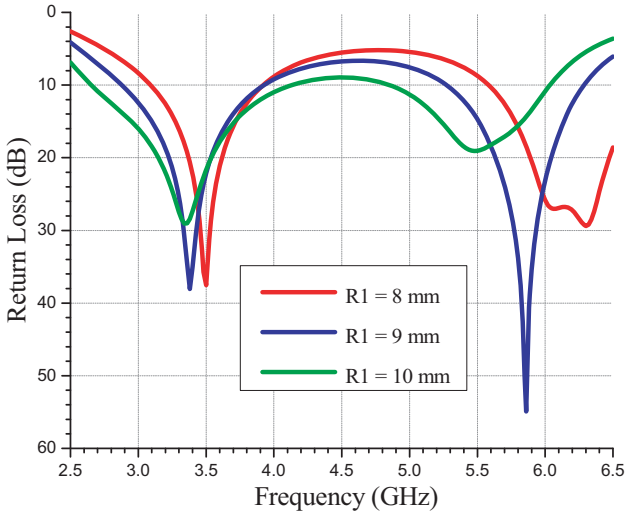

Figure 7. Return loss with variation in radius of bigger circle (R_1).

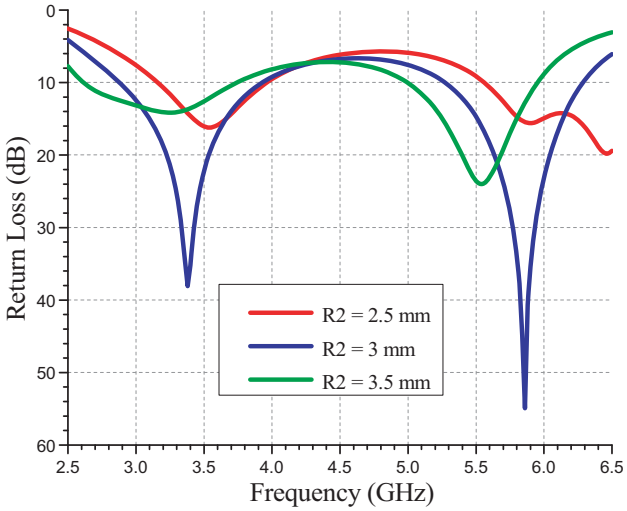

Figure 8. Return loss with variation in radius of smaller circle (R_2).

R_2 increases from 2.5 mm to 3 mm, f_1 & f_2 shift towards lower side significantly, and return loss also increases significantly at both f_1 & f_2. As R_2 further increases from 3 mm to 3.5 mm, f_1 shifts towards lower side marginally, but return loss decreases significantly while f_2 shifts towards lower side significantly, but return loss decreases significantly. Better results are obtained for $R_2 = 3$ mm.

Due to the circular slots cut in the patch, the excited patch surface current paths are lengthened, which effectively lowers the resonant frequencies [5]. It can be verified by surface current density variations of the proposed antenna (Figure 5(b)). It is clear from Figures 7 & 8 that if R_1 or R_2 increases, f_1 and f_2 shift towards lower side. This implies that, at a fixed dual-frequency operation, the required antenna size can be reduced [7]. Also, due to the symmetric shape of the circular slot cut, the frequency ratio of the two resonant frequencies is only slightly varied [8].

For the proposed antenna, we can adjust the resonant frequencies f_1 & f_2 by varying radii (R_1 & R_2) of bigger and smaller circular slots (Figures 7 & 8). An important feature of this antenna is the capability of impedance matching at both operating frequencies with a single microstrip feed.

Utilizing the inputs from above mentioned antenna analysis, the proposed antenna is designed, and

its various parameters are optimized. The detailed results of proposed antenna (design 4) are described in next section.

4. RESULTS AND DISCUSSION

The simulation analysis is carried out by using HFSS software (Ansys HFSS, version 14.0) and measurement by using Vector Network Analyzer (Agilent Technologies, Model No. E5071C). The return loss versus frequency curve of the proposed antenna is shown in Figure 9. The proposed antenna has two resonant frequencies $f_1 = 3.38$ GHz and $f_2 = 5.86$ GHz with return losses of 38.1 dB and 54.9 dB, respectively. The impedance bandwidth of the antenna in the frequency band 2.88–3.92 GHz is 31% corresponding to central frequency f_1. The impedance bandwidth of the antenna in the frequency band 5.26–6.28 GHz is 17% corresponding to central frequency f_2. The fractional bandwidth is calculated using the following equation [1]:

$$BW\,(\%) = \frac{f_H - f_L}{f_c} \times 100 \tag{3}$$

where $BW\,(\%)$ is the fractional bandwidth in percentage; f_H and f_L are the upper and lower cut-off frequencies; f_c is the central frequency of the corresponding band. At f_H and f_L, the value of return loss is 10 dB.

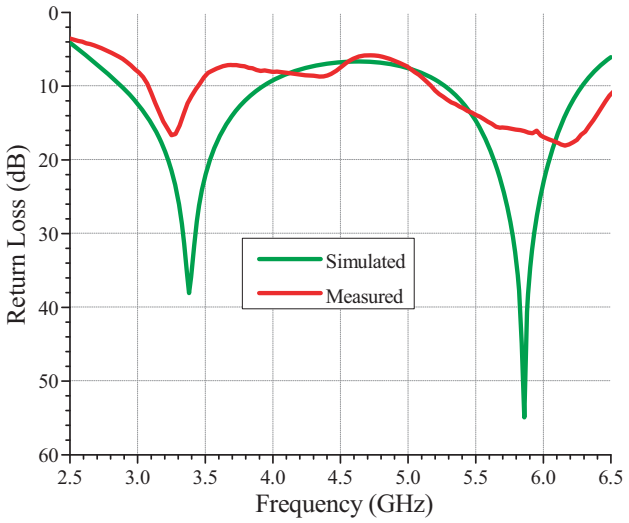

Figure 9. Return loss.

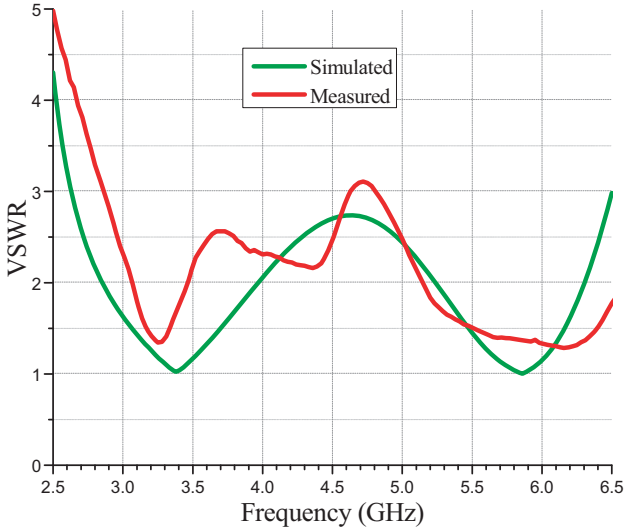

Figure 10. VSWR.

Figure 10 shows measured and simulated VSWR variations over the operating frequency bands. The values of VSWR are 1.03 and 1.01 at f_1 and f_2, respectively. This indicates that very little power is reflected back from the antenna.

Figure 11 shows the variation of total gain (simulated and measured) versus frequency curve of proposed antenna in its operating band. The simulated total gains are 3.05 dBi and 5.78 dBi at resonant frequencies f_1 and f_2, respectively, and the measured total gains are 2.96 dBi and 5.64 dBi at resonant frequencies f_1 and f_2, respectively. The total gain (G) in dB is measured by two antenna method using the following formula [1]:

$$(G)\ \text{dB} = 10\log_{10}\left[\frac{P_r}{P_t}\right] - (G_t)\ \text{dB} - 20\log_{10}\left[\frac{\lambda_0}{4\pi R}\right] \tag{4}$$

where P_t is the power transmitted by pyramidal horn antenna; P_r is the power received by antenna under test (AUT); G_t is the gain of the pyramidal horn antenna; λ_0 is the free space wavelength; R is the distance between transmitting antenna and AUT.

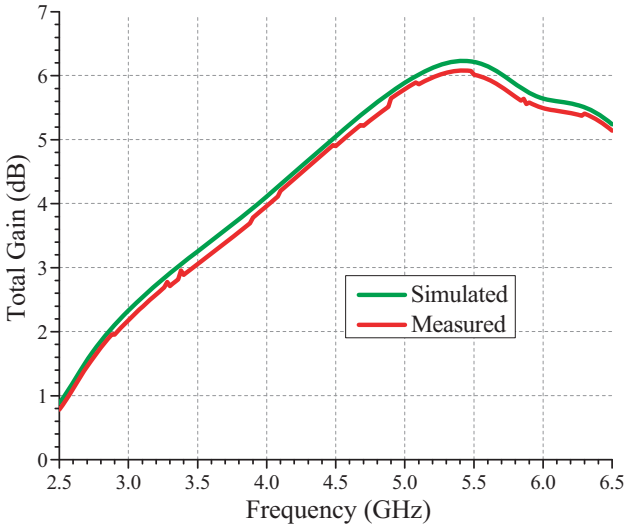

Figure 11. Total gain.

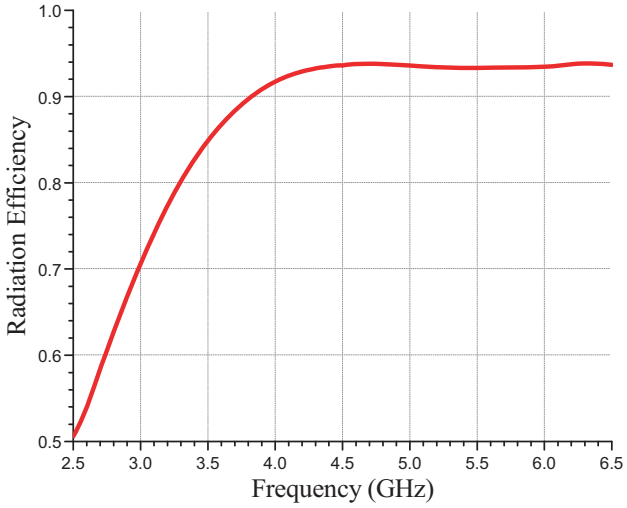

Figure 12. Radiation efficiency (simulated).

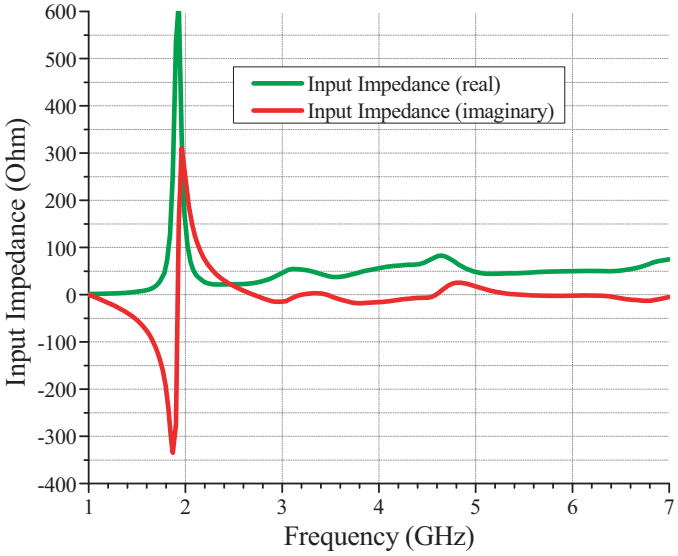

Figure 13. Input impedance (measured).

Figure 12 displays the simulated radiation efficiency over the operating frequency range. Radiation efficiencies are 82% and 93% at resonant frequencies f_1 and f_2, respectively, which indicates that the proposed antenna is able to radiate effectively.

The variation of measured input impedance (real and imaginary part) with frequency is shown in Figure 13. The input impedance of the proposed antenna is close to 50 Ω at both resonant frequencies. It is $45.58 + j3.41$ at 3.38 GHz and $49.24 - j2.32$ at 5.86 GHz, respectively.

The simulated and measured, co-polar and cross-polar, 2 D radiation patterns in E-plane (x-z plane) and H-plane (x-y plane) are shown in Figures 14(a)–(b) and 14(c)–(d) at resonant frequencies f_1 and f_2, respectively. These patterns suggest that the simulated and measured patterns are almost identical in shape. In E-plane, the antenna shows broadsided radiation characteristics while it is omnidirectional in the case of H-plane. The proposed antenna exhibits good broadsided radiation pattern with linear polarization characteristics. In E-plane, the co-polar patterns are at least 12 dB higher than cross polar patterns, while in H-plane, the co-polar patterns are nearly 10 dB higher than cross polar patterns.

The little variation in simulated and measured results (in return loss and radiation pattern) is mainly due to imperfect material, fabrication imperfections, contact losses (soldering is done to connect SMA connector to microstrip feed), cable losses, and measurement errors.

Table 2 shows a comparative study of the proposed antenna with some existing dual-band antennas on the basis of antenna size ($L \times W \times h$), dielectric constant (ε_r), lower resonant frequency (f_1), higher resonant frequency (f_2), bandwidth at lower resonant frequency (BW_1), and bandwidth at higher resonant frequency (BW_2). The proposed antenna has good combination of wider bandwidth and smaller size than all other antennas.

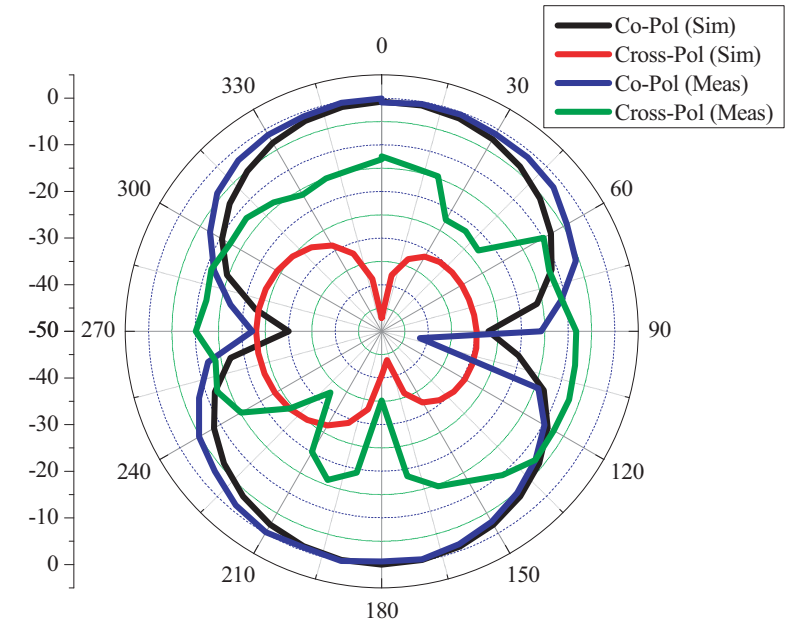

(a)

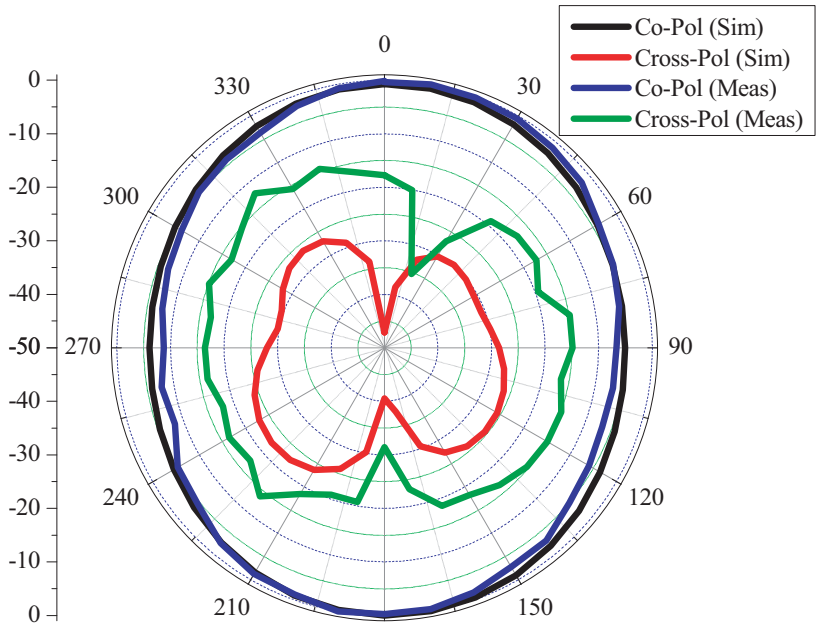

(b)

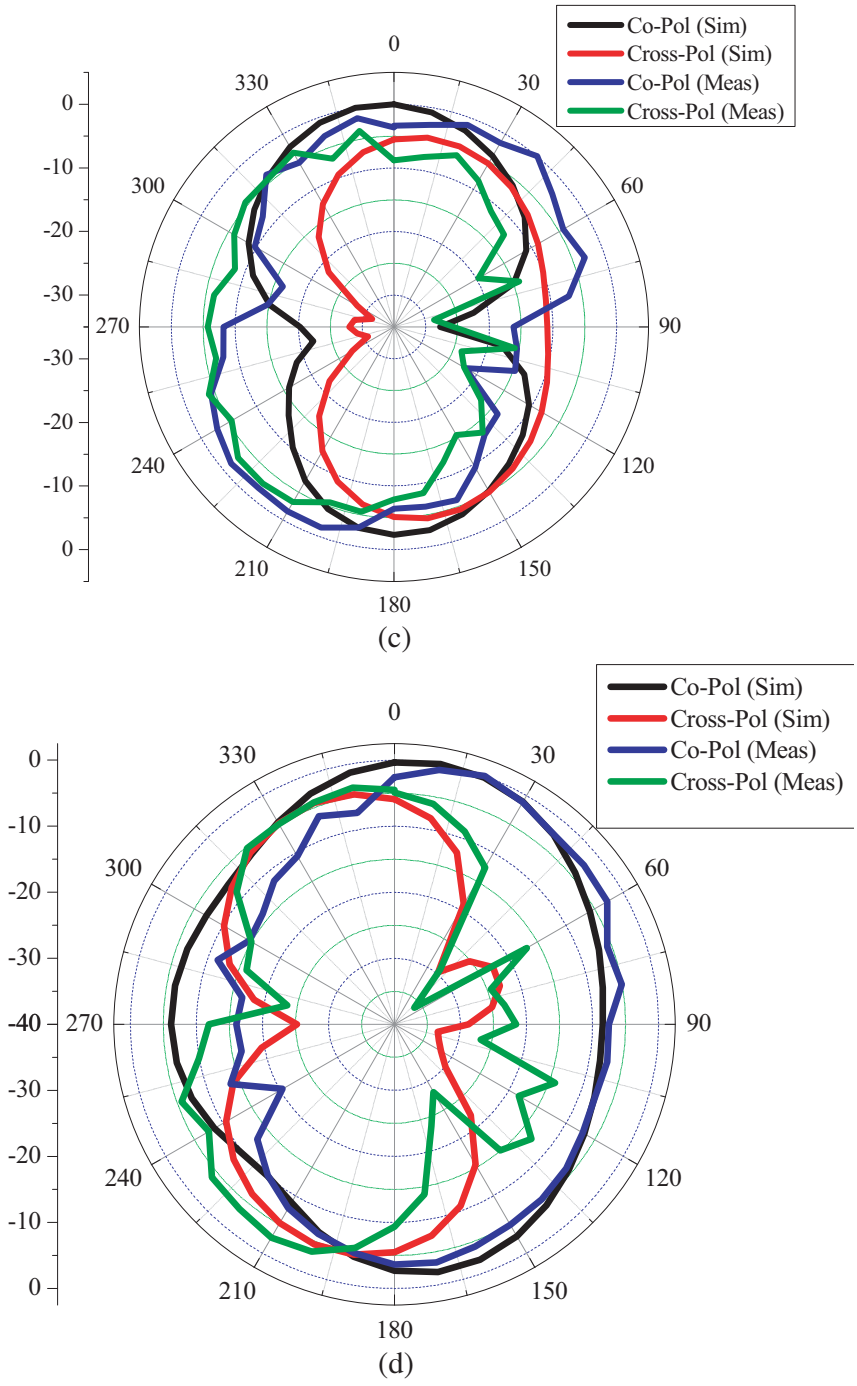

Figure 14. (a) E-plane radiation pattern at 3.38 GHz. (b) H-plane radiation pattern at 3.38 GHz. (c) E-plane radiation pattern at 5.86 GHz. (d) H-plane radiation pattern at 5.86 GHz.

Table 2. Comparison between the proposed antenna and some other dual band antennas.

Ref. No.	Overall dimension $L \times W \times h$ (mm^3)	Dielectric constant ε_r	Resonant frequency f_1 (GHz)	Resonant frequency f_2 (GHz)	BW_1 (%)	BW_2 (%)
[4]	$37.7 \times 28.4 \times 1.6$	4.4	1.8	2.3	2.05	2.44
[5]	$33.2 \times 25.5 \times 1.6$	4.4	2.155	2.714	2.0	2.4
[6]	$33.2 \times 25.5 \times 1.6$	4.4	2.155	2.698	1.9	2.2
[7]	$42 \times 42 \times 1.6$	4.4	1.731	2.003	1.8	2.15
[8]	$108 \times 108 \times 1.6$	4.4	0.83	2.705	26.2	22.2
[10]	$100 \times 120 \times 1.6$	4.4	1.575	2.4	1.6	8.4
[11]	$70 \times 70 \times 1.6$	4.4	3.1	4.7	3.2	4.2
[12]	$60 \times 60 \times 1.0$	4.4	3.3	5.6	38.8	27.5
Proposed antenna	$40 \times 40 \times 1.6$	4.4	3.38	5.86	31	17

5. CONCLUSIONS

In this article, a simple, compact, dual-band modified circular slot antenna is designed and analyzed. The proposed antenna resonates at two frequencies of 3.38 GHz and 5.86 GHz with more than 38 dB return loss at both frequencies and corresponding impedance bandwidth of 31% and 17%, respectively. Average gains of the proposed radiator are 3.0 dBi and 6.0 dBi in lower and upper frequency bands, respectively. The proposed antenna shows broadsided radiation pattern in E-plane while it is omnidirectional in H-plane. These features make it appropriate for WiMAX (3.5 GHz) and WLAN (5.8 GHz) applications.

REFERENCES

1. Balanis, C. A., *Antenna Theory, Analysis and Design*, John Wiley & Sons, 2005.
2. Garg, R., P. Bhartia, I. Bahl, and A. Ittipiboon, *Microstrip Antenna Design Handbook*, Artech House, 2001.
3. James, J. R. and P. S. Hall, *Handbook of Microstrip Antennas*, Peter Peregrines, 1989.
4. Yang, K. P. and K. L. Wong, "Inclined-slot-coupled compact dual-frequency microstrip antenna with cross slot," *Electronics Letters*, Vol. 34, No. 4, 321–322, Feb. 1998.
5. Chen, H. D., "A dual-frequency rectangular microstrip antenna with a circular slot," *Microwave and Optical Technology Letters*, Vol. 18, No. 2, 130–132, Dec. 1998.
6. Chen, W. S., "Single-feed dual-frequency rectangular microstrip antenna with square slot," *Electronics Letters*, Vol. 34, No. 3, 231–232, Feb. 1998.
7. Lu, J. H. and W. L. Wong, "Compact dual-frequency circular microstrip antenna with an offset circular slot," *Microwave and Optical Technology Letters*, Vol. 22, No. 4, 254–256, Aug. 1999.
8. Tiang, J. J., M. T. Islam, N. Misran, and J. S. Mandeep, "Circular microstrip slot antenna for dual-frequency RFID application," *Progress In Electromagnetics Research*, Vol. 120, 499–512, Oct. 2011.
9. Yang, Y. H., J.-L. Guo, B.-H. Sun, and Y.-H. Huang, "Dual-band slot helix antenna for global positioning satellite applications," *IEEE Transactions on Antennas and Propagation*, Vol. 64, No. 12, 5146–5152, Dec. 2016.
10. Hung, C. and T. Chiu, "Design of dual-band cavity-backed slot antenna loaded with spurline," *IET Microwaves, Antennas and Propagation*, Vol. 10, No. 9, 939–946, Jun. 2016.
11. Kandasamy, K., B. Majumder, J. Mukherjee, and K. P. Ray, "Dual-band circularly polarized split ring resonators loaded square slot antenna," *IEEE Transactions on Antennas and Propagation*, Vol. 64, No. 8, 3640–3645, May 2016.
12. Rui, X., J. Li, and K. Wei, "Dual-band dual-sense circularly polarised square slot antenna with simple structure," *Electronics Letters*, Vol. 52, No. 8, 578–580, Apr. 2016.